Evolutionary Adaptive Discovery of Phased Array Sensor Signal Identification

Timothy R. McJunkin and Milos Manic

Abstract— **Tomography, used to create images of the internal properties and features of an object, from phased array ultasonics is improved through many sophisiticated methonds of post processing of data. One approach used to improve tomographic results is to prescribe the collection of more data, from different points of few so that data fusion might have a richer data set to work from. This approach can lead to rapid increase in the data needed to be stored and processed. It also does not necessarily lead to have the needed data. This article describes a novel approach to utilizing the data aquired as a basis for adapting the sensors focusing parameters to locate more precisely the features in the material: specifically, two evolutionary methods of autofocusing on a returned signal are coupled with the derivations of the forumulas for spatially locating the feature are given. Test results of the two novel methods of evolutionary based focusing (EBF) illustrate the improved signal strength and correction of the position of feature using the optimized focal timing parameters, called Focused Delay Identification (FoDI).**

I. INTRODUCTION

Sensors are often thought of as statically configured devices, with the goal of gathering as much information from as many directions as possible with processing, reduction and interpretation left as a post processing task. With some highly configurable sensors, adaptive reconfiguration would be a power tools. Similar to the eye in advanced living organisms a phased array ultrasonic system can adjust gains, steer, focus, and, ultimately, be physically moved through locamotion to produce a better point of view and better analysis of the subject of interest. This paper presents an architecture and first steps to utilizing the phased array system in a way to more fully utilize the power of reconfiguration to solve ambiguities and arrive at more precise tomography providing better interface for human interaction.

Sound has long been used as a means to make measurement of our surroundings. Measuring the time of propagation of sound yields information about the proximity of objects emanating or reflecting sound. The applications range from mapping of objects in air and water to detailed examination of human tissues as a medical diagnostic technique. In the medical and industrial applications, the frequency of the acoustic waves used is typically well above the range of human hearing and is referred to as ultrasound. In a time of flight use of ultrasonics, a material such as a piezoelectric crystal is excited with a sharp pulse of electricity that causes a mechanical deformation. The mechanical energy is transferred into mechanical vibrations in a material and propagates through the material. Gases and liquids typically support a longitudinal compression and propagation only, where as solids may support transverse (also known as shear wave) oscillations and propagation. The sound propagates according to the physical properties of the material which determine the velocity of propagation and attenuation of the waves. The size and shape of the crystal determine the pressure profile. Studied as a wave energy, sound may reflect, refract or diffract to alter the path and mode of propagation when the sound approaches an area where the materials properties change (e.g. a discontinuity such as a void in a metal or hard tissue in a biological specimen). The examination of the energy returned to the crystal, which will be referred to commonly as an ultrasonic transducer or simply "transducer", gives a large amount of information about internal structures in a nondestructive manner. The direction of the sound can be assumed and when the speed of sound propagation is known, a distance measurement can determine the location of the reflection. Of course, the propagation direction of sound is not bounded to a vector. The path that the sound took in exact terms is not known. It may be slightly off angle or the result of beam spread or side lobes. This may cause the amplitude versus time information to be misinterpreted. In a solid both shear and longitudinal waves coexist traveling at different speeds, posing a potential for a large misrepresentation of a signals location.

To produce better imaging by "focusing" sound in the near field of ultrasonic transmission, phased array ultrasonics (PAU) has been developed and applied to medical and industrial applications. With this technology, the propagation of sound can be controlled to a great extent by steering, focusing at various depths, and scanning by electronically moving the aperture selected. This technology, summarized in the next subsection, has been exploited to provide extraordinary imagining and subsequent rendering to interpret the data as a realistic three dimensional view of organs or fetuses in utero. Much research has been done to produce better imaging from data collected. One solution is to collect even more data and apply sophisticated data fusion [1] and interpretation algorithms. For example linear classifiers with wavelets have been applied to make additional inference from data sets [2]. Modeling of the fields produced by phased arrays [3], provides possible amelioration of problems associated with

Work was supported by the U.S. Department of Energy through the INL Laboratory Directed Research and Development (LDRD) Program under DOE Idaho Operations Office Contract DE-AC07-05ID1417

T. McJunkin is with the Industrial Technlogy Deptartmet, Idaho National Laboratory, P.O. Box 1625 , Idaho Falls ID 83415-2210, USA timothy.mcjunkin@inl.gov

M. Manic is with the Department of Computer Science, University of Idaho, 1776 Science Center Drive, Ste.303 Idaho Falls, ID 83402, USA misko@ieee.org

grating lobe or side lobes through better design; however, the spread of sound to all connected material still presents issues in interpretation of data. Pörtzgen used wave equation based to predict artifacts created in images from alternate paths that allows removal of artifacts that match the predicted pattern [4]. Some novel litterally flexible approaches have been taken [5].

A very comprehensive way of collecting data is described by Holmes in [6], [7], [8], whereby an attempt to collect all available information from a set of array elements is completed by individually exciting each element and recording the time series response from all of the elements. In this way, reconstruction of any combination of transmit and receive elements can be post processed with arbitrary delays for examination. Methods for attempting correction due to variation in sound velocity have been developed [9], again from post processing of data. The method may put an undo burden on the amount of data collected. Also, these papers do not account for multiple modes of propagation possible. The present research describes another tool and a paradigm that will allow the sensor to overcome some basic interpretation problems and advance the full data acquisition interpretation as well as utilize more typical commercial instruments.

This paper is organized into logical sections. Section II. provides the reader with background on phased array ultrasonics and Section presents background on PAU and the concept of using it as an adaptive sensor. The novel way of indentifying the exact origin of a ultrasonic signal using phased array as an adaptive sensor using evolutionary based focusing and focused delay indentification is discussed in Section III. Section IV. presents the system setup to perform experiments on physical stainless steel blocks and the results of those experiments. Conclussion and futures direction of this method are finally given in Section V.

II. BACKGROUND

A. Phased Array Ultrasonic Tomography

A crystal can be caused to expand by applying a voltage. Conversely when a force is put on the crystal it will generate electrical energy which can be measured as a voltage. Ultrasonics utilizes the conversion of electrical energy to mechanical energy and the inverse to transmit and receive mechanical waves into a test subject. For a contiguous crystal the characteristics of the transmitted sound are determined by the size and shape of the crystal or aperture and the characteristics are fixed. For example a small aperture will look much like a point source where the sound waves will spread out in a spherical shape; visualize the ripples when a small pebble is thrown into a pond. Over time the ripple moves out at greater radii. A more complicated and very flexible and powerful configuration of many "point" sources is PAU.

In PAU, the impulse to each element is timed to point the beam in a specific direction and focus it at a particular depth. By steering the beam through a sequence of angles an image can be formed. The example in Fig. 1 shows an image taken from a scan of an aluminum plate that has been friction stir welded [10]. A delay pattern, called a focal law, to generate a sound path in a particular direction has been calculated for each angle. The acquired signal for each is in the form of the signal on the right. Coding the amplitude with color and rendering the time amplitude signal, referred to as an *A-scan*, at the appropriate angle the image is displayed. There are obvious reflectors represented in the image. There are also numerous lower amplitude signals shown through out the image. These are items may be real and in the location shown or may be shadows of the large items. The methods in this paper provide an important tool to resolve that question.

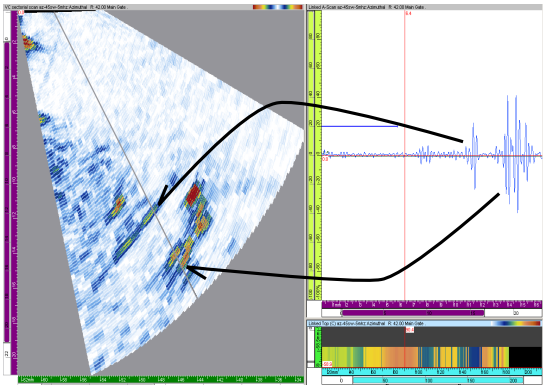

Fig. 1. Amplitude versus time signals (A-scan) shown on the right are collected at a range of angles and displayed in a typical sector scan image. Arrows show where peaks in the A-scan are displayed on the image.

B. Multiple Propagation Modes

There are numerous sounds paths that may reflect off a reflector. Fig. 2. illustrates four possible pulse echo (PE) paths that will provide a paths that focus on the same point from the same set aperture on the array. In this illustration the transducer is on a angled wedge that allows sound to propagate at a nominal angle. Note that Fig. 2 A and B have similar paths, but have a strikingly different focal law shown on the right. Observing, the signals illustrated in Fig. 3 show the timing of these possible sound paths. The important aspect of this illustration to the current work is that there is no way to know if a signal returned comes from a reflector that is close propagating as a shear wave or is farther away propagating as a longitudinal wave, which travels much faster. However, if the object is in "focus" the shape of the focal law yields the answer.

C. Adaptive Sensor Architecture

A typical PAU system connects transducer elements to both a transmit and receive multiplexer. The transmit channel contains pulsers, which produce a voltage pulse, driven by a programmable delay generator. The receive side has amplifiers then a signal delay block followed by a summation block and a digitizer. Note: digitizers could be placed after the initial amplification and the delays and summation done digitally. Behind that are registers containing the set of configuration parameters which are designed to be cycled through as fast as possible so that one cycle through all of the

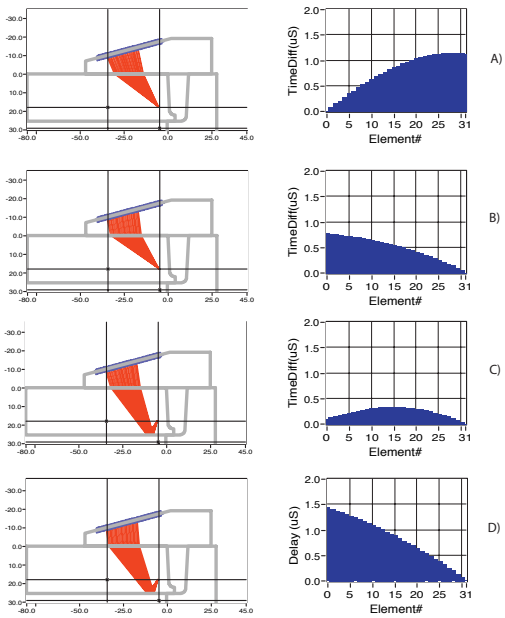

Fig. 2. Four sets of possible sound paths to a given target. A) is a focus for a shear wave on a direct path, B) for a longitudinal wave on a direct path, C) for a shear from a reflection from the bottom of the part shown, and D) a longitudinal from a reflection. Delays on the right show necessary delay patterns to achieve focus on the path.

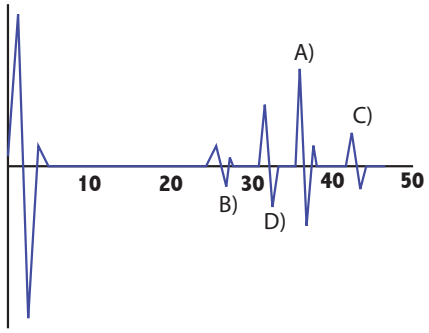

Fig. 3. An illustration of what the A-scan (i.e. amplitude versus time of the received signal) for the energy returned from the four paths shown in Fig 2. All four paths shown and others may produce signal of varying amplitudes depending on where the timing has focused the sound.

patterns can occur as close as possible to the same time. This is important when the transducer is either being moved by manual or automatic methods, so that the cross-sections are sampled at the same physical scan location. For this purpose, the architecture does not need to be optimized for reloading the configuration. The algorithms described in this paper are therefore not practical without redesign of hardware to perhaps implement the algorithms tightly integrated with the hardware. However slowly it was performed currently, the necessary architecture change to allow the data to drive the configuration of the sensor with similarity to a biological system is shown in Fig. 4. Existing systems described in the Experimental Setup section can be used to implement the shown architecture but at a low level of performance.

III. SIGNAL INDENTIFYING ALGORITHMS

In this section, two algorithms for beam focusing using evolutionary algorithms to adapt the focal law delays. One adjust each phased array individual element delasy with an independent random perturbation. The second randomly changes the physical parameters of sound speed and focus position. Both use amplitude of a signal of interest as the fitness measure.

A. Evolutionary Based Focusing

Two methods of evolutionary Based Focusing (EBF) based on randomly perturbing the delays for the focal laws are defined here. The first is completely unstructured in the sense that the expected shape of the curve formed in the delays for focusing at a particular point is neglected. The second starts with the standard form for calculating the delays for producing simultaneous arrival of the wave fronts at a desired point with a known sound speed. In both, the focusing of the phased array focal law delays on a signal of interest (SOI) is completed in an iterative self organizing manner of perturbing the delays randomly and measuring the fitness of the focus through the amplitude, measured as the difference between the absolute maximum and minimum of the SOI within the signal window. A window length was chosen based on observation to be 50 samples. Other measures of fitness are possible including the decrease in amplitude of other peaks or metrics on the shape of the SOI.

To account for possible variation in coupling due to small vibrations or drying of couplant over the potentially long periods of the experiments, the system was setup with two focal law channels, one with the current best configuration and the other with the altered configuration. The two cases would be activated within milliseconds of each to each other so the comparison would exclude anything that could be time varying. The rate at which trials could be performed was relatively slow, due to the latency to reconfigure the hardware. As suggested in the architecture section for adaptive algorithms to be put in commercial use, the hardware architecture would also have to evolve to allow those updates to occur faster. The evolutionary process is also slow requiring many iterations that did not improve fitness. Although the transmit and receive delays and the apertures used can be unique, this paper is limited to pulse echo where the send and receive delays are the same, leaving analysis for the more arbitrary case to future papers.

1) Individual Element Delays: The set of delays, t_d are associated with a linear array element position. Each delay, $t_d[i]$ is combined with the transducer element location $p[i]$, which in a linear array positioned horizontally on the part under test (PUT) is the horizontal displacement from the first element. The element position is then $p_x[i] = \Delta xi$, where Δx is the spacing, or pitch, between the center of two sequential elements. The configuration controlling the sound propagation is then determined by the ordered pairs

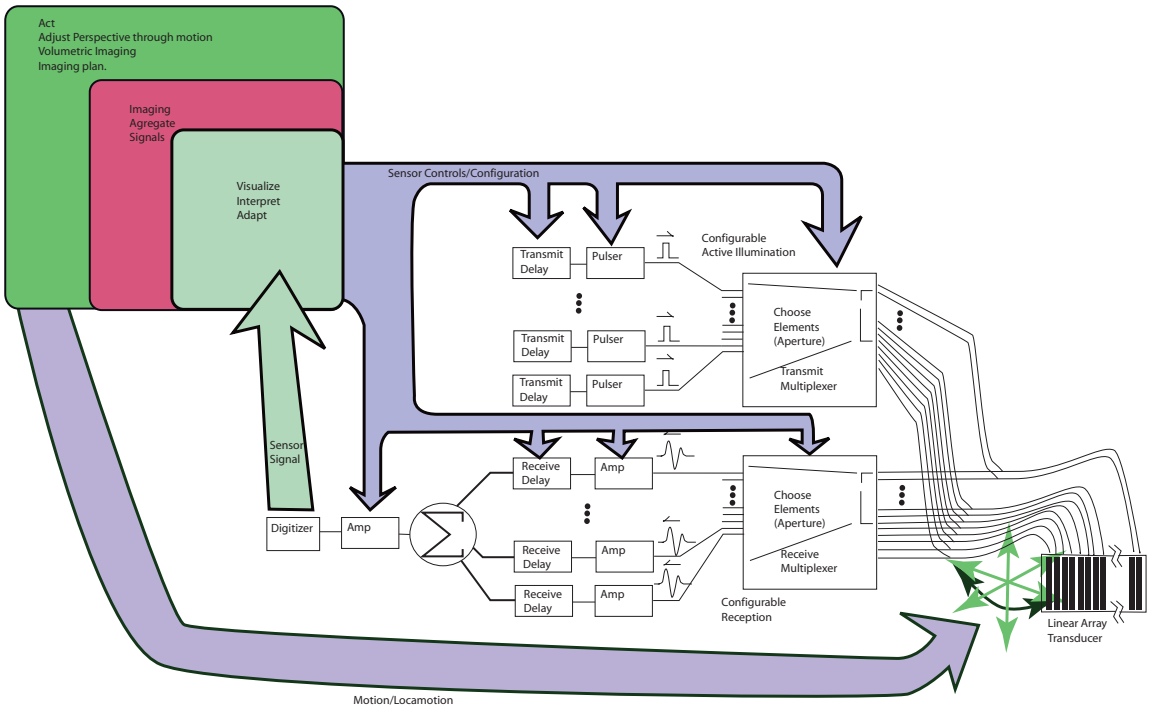

Fig. 4. A modified architecture allows algorithms to react to the data collected and extract more detailed information in area that are determined to be of interest and an physical interaction where either system or human operator repositions the sensor based on cues from the data.

of $(t_d[i], p_x[i])$. For the purpose of this paper the positions will be held constant for a given experiment but with either locomotion of the transducer or by changing the choice of element this could be utilized in the adaptations. The mutations of the evolutionary algorithm are implemented by randomly choosing a change to the delay. A maximum change is selected Δt_d and a set of random numbers for each element between 0 and 1, $r[i, n]$. A new set of delays is found This is found for $i = 1...N$ with

$$temp[i] = t_d[i, n] + r[i, n]\Delta t_d \quad (1)$$

$$t_{dm}[i] = temp[i] - \min_{j=1...N} temp[i]. \quad (2)$$

, Now each set is executed. If the result of the mutation provides greater fitness, the successful generation counter, n, is incremented and the current most optimal set of delays becomes $t_d[i, n + 1] = t_{dm}[i]$. Otherwise, the mutations are discarded. This process repeats until the fitness ceases to improve significantly. The stopping point for the current paper was arbitrary.

2) Physical Parameters: This method requires the a priori knowledge about the timing of energy propagation from the phased array elements. The form of the focal law delays given known focal point location, the sound speed and the transducer pitch is derived here, producing the expression of which a small number of parameters can be perturbed to create the mutations instead of each delay.

The concepts described here have been applied to the flexible and powerful technology of PAU. A PAU ultrasonic transducer is divided into numerous small piezoelectric-electric transducers each with its own electrical connection. The electronics connected to this transducer is designed to tightly control timing of the pulses that excite each of these elements precisely. At the first order of approximating, the individual elements are point sources for emitting mechanical force which is used to put a impulse into the subject being examined causing an acoustic wave to be propagated.The purpose in controlling and receiving point sources in concert is to guide the sound along the entended line of travel and to "focus" at a desired depth or location. The desired point of focus is achieved by producing constructive interference of the waves from each of the point sources with control of timing delays. With the known relative position of the elements and the speed of sound propagation in the material a delay for the exciting impulse to each element can be calculated for an arbitrary location in proximity to the transducer. Energy that returns to the transducer is again transformed from an acoustic wave to a mechanical deformation of the piezoelectric electric crystal, finally producing an electrical signal that can be digitized. A configuration of a linear PAU transducer is illustrated in Fig. 5, where an array is placed in direct contact with the subject material. Using Fig. 5, the basic concept can be expressed by considering the path of a wave front propagating from each of the elements used in the aperture along the red lines to a point in which focus is desired (i.e. the intersection of the lines shown).

The expression for the distance of sound propagation for each individual element to or from a point location is described simply as

$$d[i] = \sqrt{(X - i\Delta x)^2 + Y^2} \quad (3)$$

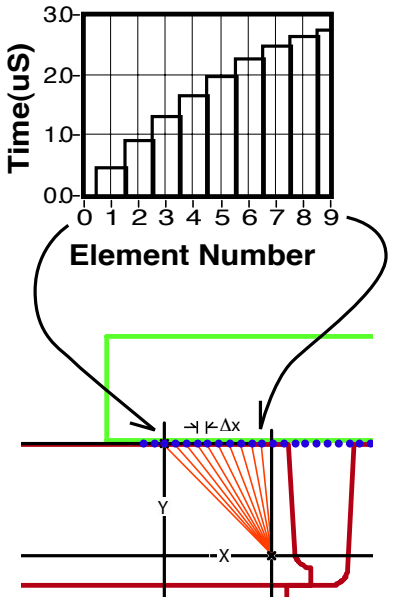

Fig. 5. Example showing a linear phased array transducer placed directly on of the sound paths from the individual elements of the transducer to the desired focal point shown with the necessary delays to each element to allow the propagating wave fronts to arrive simultaneously at that point.

$$d[i]^2 = (X - i\Delta x)^2 + Y^2 \quad (4)$$
$$= X^2 + Y^2 - 2i\Delta x X + i\Delta x^2 \quad (5)$$

where X and Y are the relative Cartesian positions of the focal point with respect to the location of the 0^{th} element of the transducer, Δx is the spacing of the transducer elements in the direction of X and i is the element number counting from 0 to $N-1$. This expression must be expressed in time to arrive at the necessary delays to produce the focusing affect. With a known sound speed, ν, time of flight to and from the elements to the focal point is

$$t[i] = d[i]/\nu \quad (6)$$
$$t[i] = \frac{\sqrt{(X - i\Delta x)^2 + Y^2}}{\nu} \quad (7)$$
$$t[i]^2 = c + bi + ai^2 \quad (8)$$

where

$$a = \left(\frac{\Delta x}{\nu}\right)^2 \quad (9)$$
$$b = -\frac{2X\Delta x}{\nu^2} \quad (10)$$
$$c = \frac{X^2 + Y^2}{\nu^2} \quad (11)$$

.

The necessary delays to focus as in Fig. 5 are found by identifying the maximum time of flight and subtracting the time of flight for each element such that the longest path pulse is triggered at $t = 0$ and each of the other elements are triggered subsequently by the calculated delay, as such:

$$t_d[i] = \max_{j=0\ldots N-1} t[j] - t[i]. \quad (12)$$

The mutations could be performed by perturbing gradually the constants $a, b$and$c$. Though, for the current experiments the choice of altering the parameters with physical meaning (X, Y, and ν) was made. As with the individual delays a random variable is produced for each parameter, $r_X[n], r_Y[n],$ and$r_\nu[n]$ to adjust the next mutations as

$$X_m = \Delta X(r_X[n] - 0.5) + X[n] \quad (13)$$
$$Y_m = \Delta Y(r_X[n] - 0.5) + Y[n] \quad (14)$$
$$\nu_m = \Delta\nu(r_X[n] - 0.5) + \nu[n]. \quad (15)$$

Using equation (8), the time of propagation for each element is determined. The final delays are found by applying (12). The focal laws are executed. If the fitness function is improved then the new parameters are maintained as $X[n+1] = X_m$, $Y[n+1] = Y_m$, and $\nu[n+1] = \nu_m$.

B. Focused Delay Indentification

Upon arriving at the focus point, through the iterative means described previously, the standard equation can be used in reverse by solving for the parameters of the standard point reflector form. The accronym for focused delay indentification is FoDI. The delay laws $t_d[i]$ must be added to the time of flight, t_f, to the start of the pulse to find the flight times $t[i]$ for the sound to and from the target that has been focused upon. Although the time of the peak or the time of the start of the window might be an acceptable choice for time of flight, a more accurate determination of the start of the packet should be determined. A matched filter tuned to the frequency of the ultrasound combined with a heuristic algorithm for following the sync function back to the start was used to find t_f. The matched filter is a three point matched filter spaced at half cycles of the center frequency of the transducer. The point of maximum correlation is associated with the peak of the three half cycles containing the peak. Repeatedly, moving earlier in time in the correlation to the next local maximum in the selection window until the next local maximum is not greater than 20% of the previous one. The time associated with the final acceptable local maximum is thus t_f.

The time of flight is that for the round trip of the sound. So the transit time from or to the target to each of the elements is

$$t[i] = t_f/2 + t_d[i] \quad (16)$$

. With numerous elements the solution of the three unknown constants (a, b, and c) can be solved in a least squares manner. The means squared error of the least squares solution may serve as a possible measure of the convergence.

The solution for the constants can be converted through solving the expressions (9), (10), and (11) for the physical parameters:

$$\nu = \sqrt{a}/\Delta x \quad (17)$$
$$X = b\nu^2/2\Delta x \quad (18)$$
$$Y = \sqrt{c\nu^2 - X^2}. \quad (19)$$

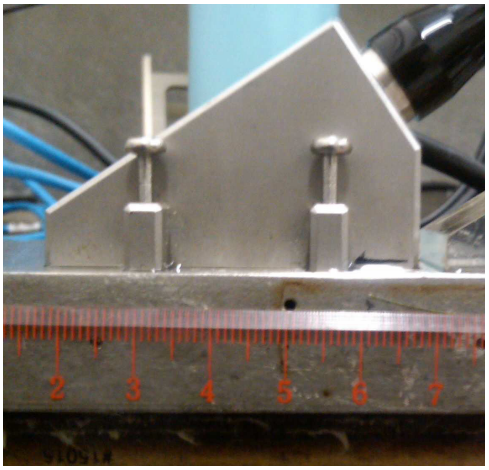

Fig. 6. Photo graph of a sixty-four element transducer placed directly on a stainless steel sample with features such as side-drilled holes shown.

If the expected shear and longitudinal sound speeds of the material are known, another measure of convergence is the proximity of ν to one of these sound speeds. The result provides a new tool for precisely determining source of the returned signal in the pulse echo mode.

An additional tool used for visualization is a wave propagation graph. Semi-circles are plotted about the transducer element locations at a radius equal to the distance traveled in $0.5t_f$ minus the delay to the transducer. This shows the location of the wave fronts. The more tightly compact the locations of the intersections of these semi-circles the closer to convergence on a point source. For this paper this is left as a qualitative measure.

IV. Experimental Setup and Results

This section describes the experimental setup used to validate the algorithms. The algorithms were demonstrated with phased array hardware and blocks. A result for determining an accurate origin of a signal for each of the two methods of focusing are presented.

A. Experimental Setup

This section describes the setup for the experiment and the equipment and software used of the development and experiments. The phased array hardware is the Focus LT by Olympus NDT, that can support 128 individual transducer elements with apertures of up to 32 elements on each transmit and receive channels. The transducer used was a 64 element linear array with center to center spacing (pitch) of $0.75mm$. For the experiments here the transducer was in direct contact with the part under test with a gel couplant used to efficiently couple energy from the transducer to the part. Fig. 6 shows a photo graph of a typical set up with the transducer on a 316 series stainless block with calibration features such as side drill holes and notches. The block is nominally $19mm$ thick.

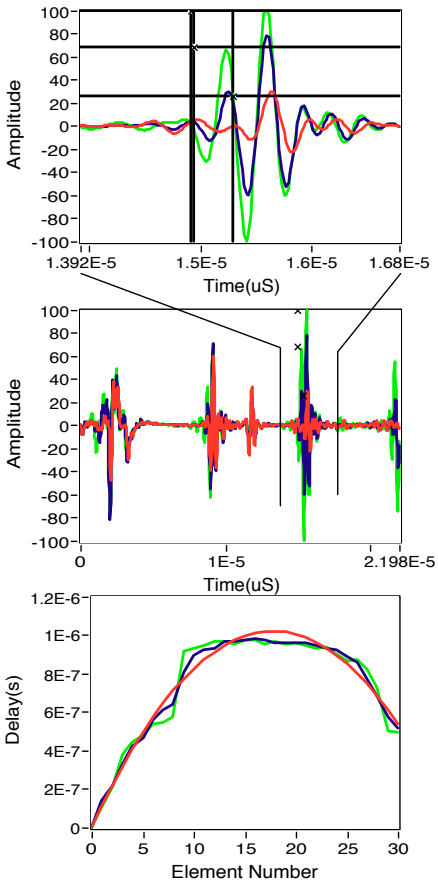

Fig. 7. Example of genetic algorithm focusing with each elements delay as possible mutation. An increase in amplitude or fitness is achieved with the flattening of the focal law delay curve. Since the reflecting surface is large and flat this is an intuitive solution. Note: signals due to reflectors other than the one of interest will decrease in amplitude.

B. Results

Results of experimental runs using FoDI are shown for both variations of EBF the individual delay method and for the parameter variation method discussed in Section III. Trials have been conducted with these method using the setup described with the transducer placed on the block in an arbitrary proximity to the side drill holes in the block. The experiments thus far have been chosen ad hoc with a starting condition of the focal law for one channel. Typically a small signal transient compared to the larger signal was chosen and the start of the window set at the beginning of it. The algorithms would be run until the amplitude of the signal achieved a significantly higher amplitude. The amplitude versus time signal for the current best case and the trial case were recorded on each successful improvement in the amplitude. The focal law delays were also recorded. The trials could then be displayed and analyzed. One result for each type is shown here to illustrate feasibility and utility. Results are presented with graphs of the amplitude versus time signal signal over the experimental run. The signals

and focal law delays is shown the start, middle and end of the experiment to illustrate the progression

1) Individual Delays: The result for the individual random delays method is shown here. The initial focus is at an off normal angle but essentially focused on the back wall ($19mm$ thick), in the shear wave mode. The result of focusing on a very large target with the individual delays is the beginning of a flattening out of the focal law curve as shown in Fig. 7. This is somewhat intuitive in that even a completely flat set of delays would provide a large amount of return back to the transducer at the same time. Although the curve fit does not work well, the approximate location of the reflector is still predicted with some error as shown by the small cross-hair in Fig. 8. The wave propagation shows a horizontal surface line of intersection at the $19mm$ back wall depth. This shows the potential for an amorphous type of focusing. It should be noted that convergence with individual delays can take thousands of iterations and is not likely practical in a real time application but does show that focusing can be achieve through a very naive technique. The maximum delay change was set to $\Delta t_d = 10ns$.

2) Physical Parameter : The example result shown for the method of varying individual parameters, produced results in far fewer iterations as shown in Fig. 9. The starting point was for a point solved for a focus of a coordinate of $(19.33mm, 10.34mm)$ and a sound speed of $4.4mm/\mu s$. Maximum changes were chosen as $1mm$ for the horizontal and vertical position and $0.1mm/\mu s$ for the velocity parameter. The experiment converged to a coordinate of $(19.54mm, 13.37mm)$ and a sound speed of $5.6mm/\mu s$. The target in this case was the 3/4 depth target centered at a depth of approximately $14.25mm$. With the diameter of the side drill hole at close to $2mm$ the approximate is reasonable. Here convergence had slowed but did continued. Actual longitudinal sound speed in this steel is approximately $5.8mm/\mu s$. This exemplifies the ability to correct the positioning of a small signal with these methods. The convergence is illustrated in the final wave propagation graphic in the upper right of Fig. 9. The source of the signal is thus effectively determined to be off axis from the center line that would normally be used to create the image. Here the image could be adjusted.

V. CONCLUSIONS AND FUTURE WORK

Conclusions and follow on work on EBF and FoDI are discussed in this section.

A. Conclusions

EBF combined with FoDI described in the paper form the basis for a new powerful tool for the nondestructive examination community. The paper describes the orignal contribution to the computational intelligence community and nondesctive examination comunity by providing the means to identify the specific origin of an arbitrary pulse echo signal without assuming a sound speed. Using these evolutionary algorithm based focusing techniqes and derived inverse focal law equations, a system can provide the exact source of a indication (i.e. reflection) automatically. This can improve tomographic data by correcting the position or eliminating artifacts in rendered images of the data. If implemented in hardware and firmware, a nondestructive examination technician could resolve previously enigmas in an ultrasonic signal.

B. Future Work

There are many avenues to take these algorithms. The most pressing is the improvement of the speed of convergence. The wave propagation graphs give a clue for a more intelligent search for the the paths that may lead to improved convergence rate. If the possible sound speeds for the material are known this these graphs give a clue in the groupings of the intersection of the propagation curves to what should be tried.

VI. ACKNOWLEDGMENTS

The authors are grateful for the assistance of Olympus-NDT, particularly for allowing the use of the beta version of Tomoview to allow software control over individual delays in focal laws through a software interface. A special thanks to Michael Moles of OlympusNDT and the University of Toronto for providing comments and insight on the draft of this paper.

REFERENCES

[1] Z. Liu, D. S. Forsyth, J. P. Komorowski, K. Hanasaki, and T. Kirubarajan, "Survey: State of the art in NDE data fusion techniques," *IEEE Transactions on Instrumentation and Measurement*, vol. 56, no. 6, pp. 2435–2451, DEC 2007.

[2] E. Moura, R. Silva, M. Siqueira, and J. Rebello, "Pattern recognition of weld defects in preprocessed TOFD signals using linear classifiers," *Journal of Nondestructive Evaluation*, vol. 23, no. 4, pp. 163–172, DEC 2004.

[3] J. Huang, P. Que, and J. Jin, "A parametric study of beam steering for ultrasonic linear phased array transducer," *Russian Journal of Nondestructive Testing*, vol. 40, no. 4, pp. 254–259, APR 2004.

[4] N. Pörtzgen, D. Gisolf, and D. J. Verschuur, "Wave equation-based imaging of mode converted waves in ultrasonic NDI, with suppressed leakage from nonmode converted waves," *IEEE Transactions on Ultrasonics, Ferroelectrics and Frequency Control*, vol. 55, no. 8, pp. 1768–1780, AUG 2008.

[5] C. R. Bowen, L. R. Bradley, D. P. Almond, and P. D. Wilcox, "Flexible piezoelectric transducer for ultrasonic inspection of non-planar components," *Ultrasonics*, vol. 48, no. 5, pp. 367–375, SEP 2008.

[6] C. Holmes, B. W. Drinkwater, and P. D. Wilcox, "Advanced post-processing for scanned ultrasonic arrays: Application to defect detection and classification in non-destructive evaluation," *Ultrasonics*, vol. 48, no. 6-7, pp. 636 – 642, 2008, selected Papers from ICU 2007. [Online]. Available: http://www.sciencedirect.com/science/article/B6TW2-4T84JYC-1/2/18e984fe49f080ed972622bd232eaf45

[7] ——, "Post-processing of the full matrix of ultrasonic transmit-receive array data for non-destructive evaluation," *NDT & E International*, vol. 38, no. 8, pp. 701 – 711, 2005. [Online]. Available: http://www.sciencedirect.com/science/article/B6V4C-4GDBT81-1/2/a0bdf4643018ce41ec312997f2fc0fb2

[8] C. Holmes, B. Drinkwater, and P. Wilcox, "Post-processing of ultrasonic phased array data for optimal performance," *Insight*, vol. 47, no. 2, pp. 88–90, FEB 2005.

[9] M. O'Donnell and S. Flax, "Phase-aberration correction using signals from point reflectors and diffuse scatterers: measurements," *IEEE Transactions on Ultrasonics, Ferroelectrics and Frequency Control*, vol. 35, no. 6, pp. 768–774, Nov 1988.

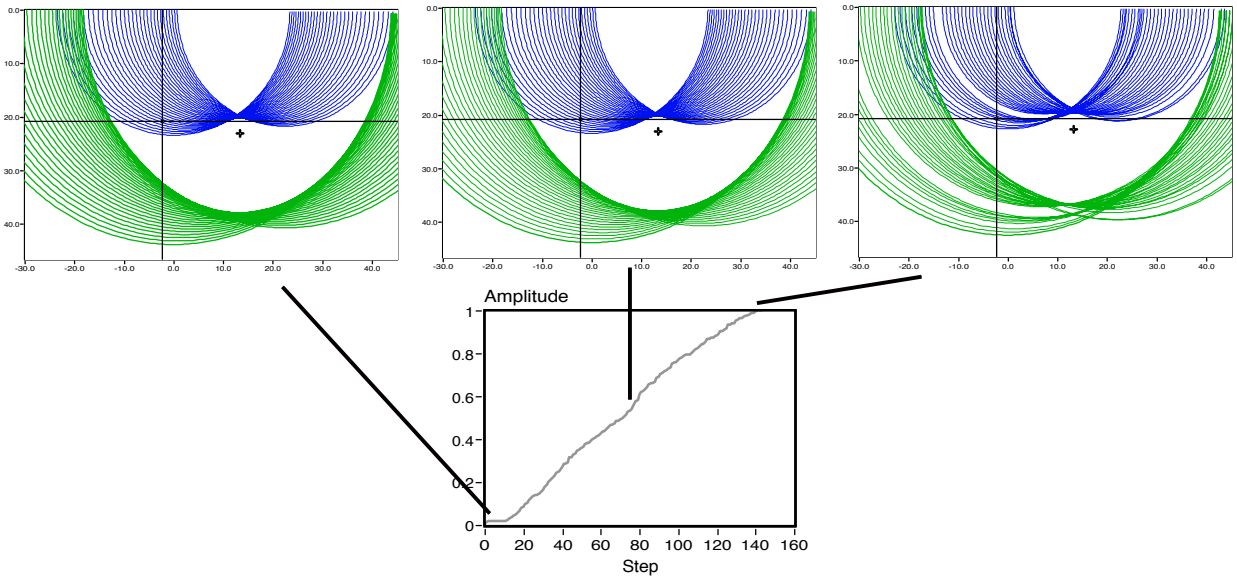

Fig. 8. The wave propagation of the two modes of travel expected sounds speeds are plotted. A semi-circle of the given radius for the travel given the time of flight for each element (i.e. overall time of flight minus the delay to that element) is plotted. The figure shows the amplitude increasing an the more spatially compact intersection of the delay formed ripples on the upper set of semicircles.

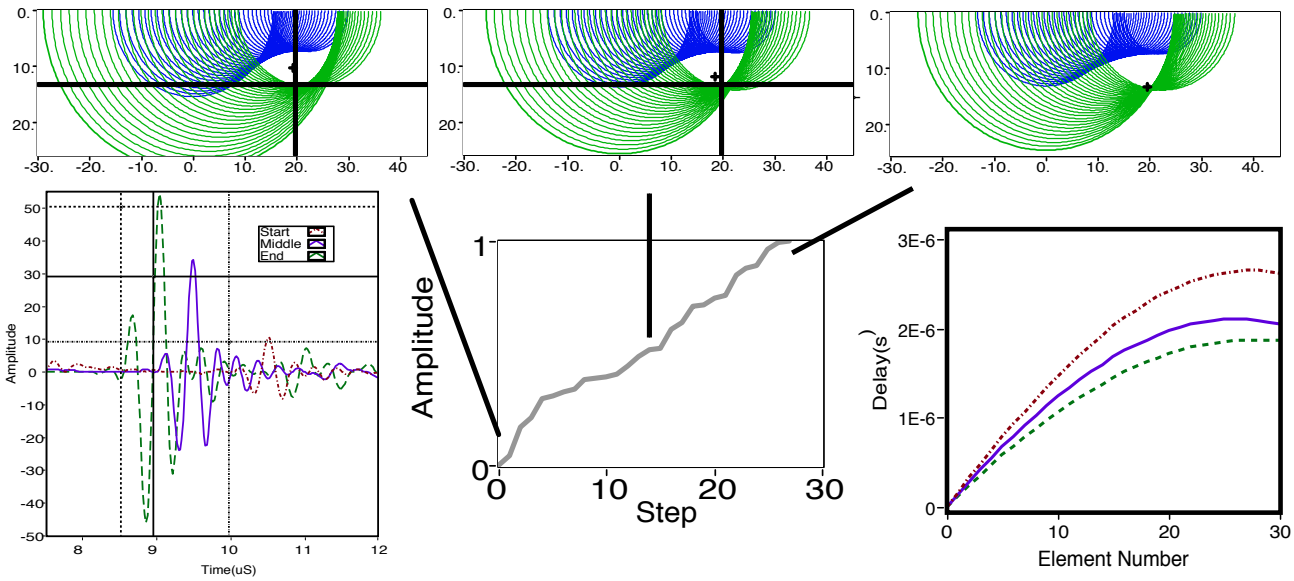

Fig. 9. The top sequence shows the convergence of the wave propagation to the higher velocity longitudinal wave. The long cursor in the right pane was removed from the graphic because it obscured the parameter fit position. The A-scan progression is shown on the lower left with the resulting focal laws in the lower right.

[10] K. S. Miller, C. R. Tolle, D. E. Clark, C. I. Nichol, T. R. McJunkin, and H. B. Smartt, "Investigation into interface lifting within FSW lap welds," in *Proceedings of the 8th International Confereence Trends in Welding Research*, S. A. David, T. DebRoy, J. N. DuPont, T. Koecki, and H. B. Smartt, Eds., 2008, pp. 133–139.